

Global control system and plasma dynamics distinguish naturally occurring and pellet-precipitated edge localized modes in the JET tokamak

S C Chapman¹, R O Dendy^{2,1}, P T Lang³, N W Watkins^{1,4}, M Romanelli², T N Todd² and JET Contributors*

EUROfusion Consortium, JET, Culham Science Centre, Abingdon OX14 3DB, UK

¹*Centre for Fusion, Space and Astrophysics, Department of Physics, University of Warwick, Coventry CV4 7AL, UK*

²*CCFE, Culham Science Centre, Abingdon, Oxfordshire OX14 3DB, UK*

³*Max-Planck-Institut für Plasmaphysik, Boltzmannstraße 2, 85748 Garching, Germany*

⁴*Centre for Analysis of Time Series, London School of Economics, London WC2A 2AE, UK*

*See the Appendix of F Romanelli *et al.*, Proc. 25th IAEA Fusion Energy Conf. 2014, St Petersburg, Russia

1. Introduction

A promising method for mitigating ELMs is to trigger smaller, more frequent ELMs by injecting pellets of frozen deuterium that modify the plasma edge[1-3]. Here, we report direct validation[4] of pellet mitigation, by identifying how to distinguish ELMs that are precipitated by pellets from natural ELMs that happen to occur at the pellet injection time. We exploit recent advances in quantitative statistical and time-domain characterization of ELMing[5-11] in tokamak plasmas. In particular, we build on our identification[8-11] of a signature of the build-up to naturally occurring ELMs. This signature was found in the instantaneous phase of the current in full flux loops in the steady H-mode of JET tokamak plasmas, when there were no attempts to trigger the ELMs. Here, in a JET plasma with both pellet injection and naturally occurring ELMs, we find the same build-up to all the naturally occurring ELMs; in contrast, all ELMs that immediately follow a pellet do not correlate with this signal phase and are thereby physically distinguishable. The plasma is actively maintained by a control system that includes global toroidal fast radial magnetic field coils near the plasma boundary. We find that the current in these control system coils also contains the build-up signature to naturally occurring ELMs, but not for pellet-precipitated ELMs. This supports the wider conjecture[9-11] that naturally occurring ELMs are precipitated by global plasma dynamics emerging from nonlinear feedback between plasma and control system.

2. Distinguishing pellet-precipitated ELMs from naturally occurring ELMs

Statistically significant information on the occurrence times of natural ELMs was previously found[8-11] in the phase of the current signals from the full flux loops in the divertor region of JET, which are a system-scale toroidally integrating diagnostic. The signal phases $\phi(t)$, derived[8,11] from the Hilbert transform of the measured timeseries $S(t)$ which yields $S(t) = A(t)\exp[i\phi(t)]$, align to the same value on a timescale $\sim 2ms$ to $5ms$ before each natural ELM occurs. We show here that this phase alignment provides a means to distinguish ELMs that occur naturally from ELMs that are triggered by pellets. Focusing on JET plasma 86908, during which both types of ELM are seen, we perform direct time domain analysis of data

from two sets of azimuthal coils for which there are high time resolution signals. The first set comprises full flux loops VLD2 and VLD3 in the divertor region in JET; their currents are proportional to the voltage induced by changes in poloidal magnetic flux. The second set is the current in the fast radial field coils (IFRFA), which are actively used for vertical stabilization of the plasma by the control system[12]. Taken together, these capture aspects of the perturbation from the control system and of the active global plasma response. A fiducial marker for each ELM occurrence time is provided by the peak[8,11] of the Be II signal. Shortly after each ELM there is a large amplitude excursion in the VLD2,3 and IFRFA signals, followed usually by non-periodic oscillations; see Fig.1.

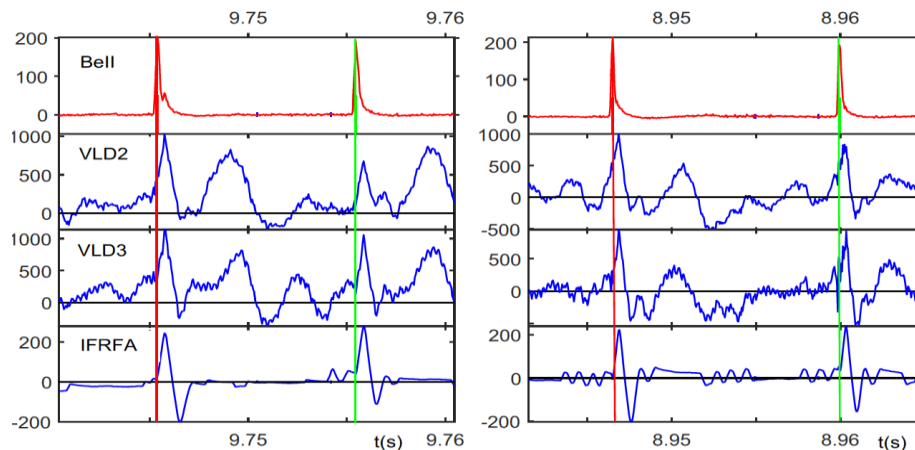


Fig.1: Standardized timeseries for two pairs of successive ELMs in JET plasma 86908. From top: Be II intensity (red), full flux loops VLD2 and VLD3, and IFRFA. To facilitate comparison we have standardized the signal amplitudes. ELM occurrence times are indicated by vertical red and green lines.

Fig.2 plots the instantaneous amplitude and phase of the VLD3 timeseries at the time of the second ELM as defined by the peak in the Be II signal. The vertical sequence of pairs of panels in Fig.2 shows VLD3 phase at times dt progressively earlier than the ELM time defined by the Be II peak. Phase bunching for the natural ELMs is visually evident at 4ms before the ELM. Detailed analysis shown in Fig 3 [4,11] shows statistically significant phase bunching up to $\sim 5ms$ before the ELM which is also seen in the IFRFA. Phase differences are calculated with respect to the occurrence time of the first ELM in the entire sequence. We find clear phase bunching for all natural ELMs in the flat-top period of H-mode in JET plasma 86908; see the upper panels in each of the four pairs of panels in Fig.2. Natural ELMs are more likely to occur when phases of these signals are at a specific value. This phase relationship is stable throughout the duration of the flat-top plasma, we have examined all ELMs that occur between 8.5s and 13.8s. In contrast, we find[4] that the ELMs directly following a pellet show no such phase bunching; see the lower panels in each of the four pairs of panels in Fig.2. The rise time of the VLD3 and IFRFA response to the ELM is fast enough that it is possible that VLD3 is already responding to the ELM by the time the Be II reaches its peak. We verified that, nevertheless, the VLD3 phase at the ELM time is not dominated by its response to the ELM, by inspecting the instantaneous amplitude[12].

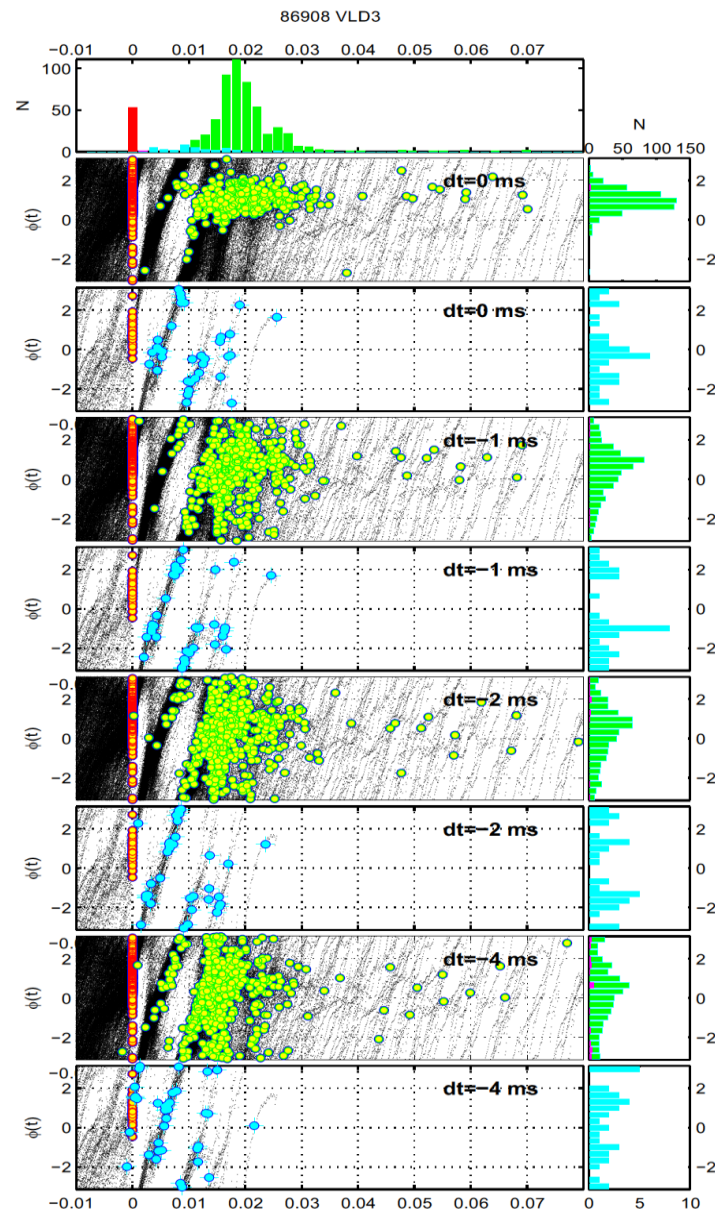


Fig.2: VLD3 temporal analytic phase at the occurrence times of all ELMs (blue circles for the first ELM following a pellet, green circles for natural ELMs) in the flat-top of JET plasma 86908, overplotted on time evolving VLD3 temporal analytic phase (black traces). Main panels: VLD3 instantaneous temporal analytic phase, modulo 2π , plotted as a function of time following each ELM (red circles) up to the occurrence time of the next ELM (blue or green circles). The horizontal coordinate is time $\delta t = t - t_0$ and the vertical coordinate is the relative phase $\delta\phi = \phi - \phi_0$ where $t_0 = t_{ELM1}$ and ϕ_0 is the phase at which the first ELM in the entire sequence occurs. Right panels: histogram of VLD3 $\delta\phi$ at the time of all the second ELMs, plotted separately for natural (green) and pellet-precipitated (blue). Top panel: histogram of ELM occurrence times for the first ELM (red) and the second ELMs (blue and green). The frequency N of first ELM times has been rescaled by $1/10$.

We previously identified a distinct new category, denoted prompt ELMs, and the timeseries in Fig.2 also show that prompt ELMs occur at a specific phase in the VLD3 response to the previous ELM. This phase relationship is seen in the $dt = -2ms$ panel of Fig.2. The prompt ELMs occur at a different phase from the non-prompt ELMs.

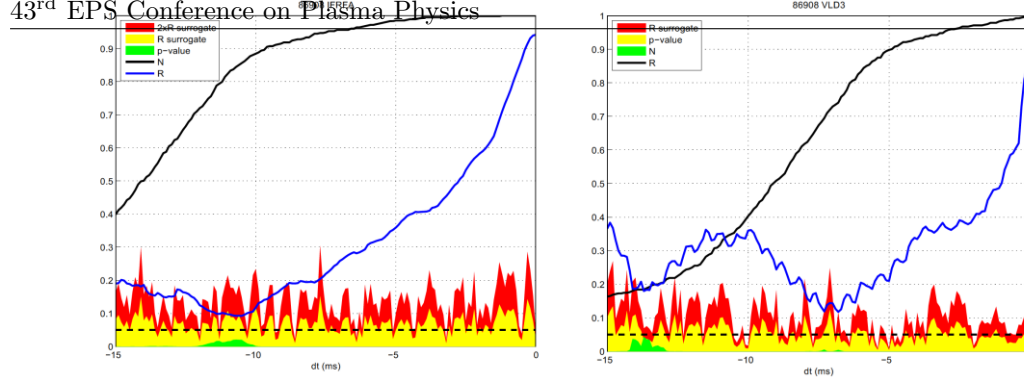


Figure 3 Rayleigh statistic for the set of all natural ELMs in the flat-top of JET plasma 86908 plotted for (left) VLD3 and (right) IFRFA phase difference $\delta\phi$ at time dt before a natural ELM. Rayleigh's R quantifies how aligned a set of phases are, $R=1$ indicating complete alignment; see [11] for details. We plot R for the original timeseries (blue line) and, to indicate statistical significance, for a surrogate where the timeseries has been randomly shuffled; yellow shading is the surrogate R value and red shading 2R. The fraction of the total set of ELMs in the analysis is plotted with a black line. The corresponding p-value (see [11]) is indicated by the green filled shading, $p=0.05$ indicated by the horizontal dashed black line corresponds to phases distributed uniformly and randomly.

3. Conclusions

For naturally occurring ELMs, the phases of the global full flux loop[8,11] and IFRFA signals contain precursor information: during $\sim 2ms$ to $5ms$ before each non-prompt ELM, the signal phase aligns to the same value. In contrast, we find[4] that ELMs immediately following pellets do not exhibit this phase alignment. Our results show that a rigorous distinction between pellet-triggered ELMs and naturally occurring ELMs can be constructed from this newly identified fact[4]. This also lends support to the suggested scenario[9-11] for naturally occurring ELMs, whereby the plasma and its interacting environment, including the control system, together self-generate a global plasma perturbation. If this perturbation is sufficiently great to modify conditions at the plasma edge for instability, a natural ELM results.

This project has received funding from the European Union's Horizon 2020 research and innovation programme under grant agreement number 210130335 and from the RCUK Energy Programme [grant number EP/I501045]. This work has been carried out within the framework of the EUROfusion Consortium and has received funding from the Euratom research and training programme 2014-2018 under grant agreement No 633053. The views and opinions expressed herein do not necessarily reflect those of the European Commission.

- [1] P T Lang, K Bich, M Kaufmann, R S Lang, V Mertens *et al.*, Phys. Rev. Lett. **79** 1487 (1997)
- [2] P T Lang, B Alper, L R Baylor, M Beurskens, J G Cordey *et al.*, Plasma Phys. Contr. Fusion **44** 1919 (2002)
- [3] P T Lang, A W Degeling, J B Lister, Y R Martin *et al.*, Plasma Phys. Contr. Fusion **46** L31 (2004)
- [4] S C Chapman, R O Dendy, P T Lang *et al.*, Nucl. Fusion, submitted (2016)
- [5] J Greenhough, S C Chapman, R O Dendy and D J Ward, Plasma Phys. Contr. Fusion **45** 747 (2003)
- [6] F A Calderon, R O Dendy, S C Chapman, A J Webster, B Alper *et al.*, Phys. Plasmas **20** 042306 (2013)
- [7] A J Webster, R O Dendy, F A Calderon, S C Chapman *et al.*, Plasma Phys. Contr. Fusion **56** 075017 (2014)
- [8] S C Chapman, R O Dendy, T N Todd, N W Watkins *et al.*, Phys. Plasmas **21** 062302 (2014)
- [9] S C Chapman, R O Dendy, A J Webster, N W Watkins, T N Todd *et al.*, Proc. 41st EPS Conf. Plasma Phys. (2014), paper P1.010 <http://ocs.ciemat.es/EPS2014PAP/pdf/P1.010.pdf>
- [10] S C Chapman, R O Dendy, N W Watkins, T N Todd *et al.*, Proc. 42nd EPS Conf. Plasma Phys. (2015), paper P2.134 <http://ocs.ciemat.es/EPS2015PAP/pdf/P2.134.pdf>
- [11] S C Chapman, R O Dendy, T N Todd, N W Watkins *et al.*, Phys. Plasmas **22** 072506 (2015)
- [12] A Murari, F Pisano, J Vega, B Cannas, A Fanni *et al.*, Plasma Phys. Contr. Fusion **56** 114007 (2014)